

Saturation magnetostriction and its low-temperature variation inferred for natural titanomaghemites: implications for internal stress control of coercivity in oceanic basalts

J. P. Hodych¹ and J. Matzka²

¹Department of Earth Sciences, Memorial University of Newfoundland, St. John's A1B 3X5, NF, Canada. E-mail: jhodych@mun.ca

²Department of Earth and Environmental Sciences, Geophysics Section, Ludwig-Maximilians-Universität München, Theresienstr. 41, München 80333, Germany. E-mail: matzka@lmu.de

Accepted 2004 January 9. Received 2003 December 12; in original form 2002 June 28

SUMMARY

Highly oxidized titanomaghemite in oceanic basalts often carries remanent magnetization of high coercivity (stability), helping preserve the oceanic magnetic anomaly pattern. We study the source of this high coercivity in four oceanic basalts (from ODP sites 238, 572D, 470A and 556) containing highly oxidized titanomaghemite (titanium content parameter $x \approx 0.55$ and oxidation parameter $z \approx 0.9$ on average). Most of the titanomaghemite is likely in single-domain grains with uniaxial anisotropy because the ratio of saturation remanence J_{RS} to saturation magnetization J_S approaches 0.50 ($J_{RS}/J_S = 0.46$ on average). We show that the uniaxial anisotropy is very likely magnetostrictively controlled through internal stresses σ_i in the titanomaghemite grains. This allows us to use a novel indirect method to estimate the saturation magnetostriction λ_S of the titanomaghemite. A saturation remanence J_{RS} is given along the axis of a cylindrical sample of each basalt. Then a small compression σ is applied repeatedly along this axis and the reversible change ΔJ_{RS} in J_{RS} is measured. Combining equations from single-domain theory for this piezomagnetic effect and for the sample's coercive force H_C gives $\lambda_S = 1.39 H_C J_S \frac{1}{\sigma} \frac{\Delta J_{RS}}{J_{RS}}$ (using cgs units, or with H_C in mT, J_S in $\frac{\text{kA}}{\text{m}}$ and σ in Pa). This yields four λ_S estimates (with *ca* 50 per cent expected error) ranging from 3×10^{-6} to 10×10^{-6} and averaging 6×10^{-6} . Theory for the piezomagnetic effect yields four σ_i estimates averaging 2×10^8 Pa. This is similar to the internal stress magnitude thought to be responsible for the high coercivity of ball-milled single-domain titanomagnetite ($x \approx 0.6$) and natural single-domain haematite. We also show that cooling to 120 °K causes $H_C J_S$ for each oceanic basalt to vary in approximate proportion to $(1 - \frac{T}{T_C})^n$ with n between 1.9 and 2.0 (where T is temperature and T_C is Curie point, both in °K). This implies that λ_S of titanomaghemite with $x \approx 0.55$ and $z \approx 0.9$ also varies in approximate proportion to $(1 - \frac{T}{T_C})^n$ with n near 1.9 or 2.0 on cooling to 120 °K (assuming that σ_i remains constant on cooling). Our results support the hypothesis that coercivity (magnetic stability) is often magnetostrictively controlled by internal stresses in the highly oxidized titanomaghemites typical of oceanic basalts older than *ca* 10 Myr. We suggest that this hypothesis can be further tested by more extensive observation of whether cooling to 120 °K often causes $H_C J_S$ of such basalts to vary in approximate proportion to $(1 - \frac{T}{T_C})^n$ with n near 1.9 or 2.0.

Key words: coercivity, magnetostriction, oceanic basalt, titanomaghemite.

1 INTRODUCTION

Titanomagnetite $\text{Fe}_{3-x}\text{Ti}_x\text{O}_4$ with $x \approx 0.6$ is the most abundant primary magnetic mineral of oceanic basalts and oxidizes gradually to titanomaghemites (Prévoit *et al.* 1968; Irving 1970; Johnson & Hall 1978; Petersen *et al.* 1979). The degree of this low-temperature oxidation is given by the oxidation parameter z , which is defined as the ratio of oxidized Fe^{2+} to originally present Fe^{2+} (O'Reilly

& Banerjee 1966) and ranges from 0 (non-oxidized) to 1 (fully oxidized).

Titanomagnetite ($x \approx 0.6$, $z \approx 0$) is an important carrier of remanent magnetization in young basalts near oceanic ridges. Its saturation magnetization J_S , magnetocrystalline anisotropy constant K_1 and saturation magnetostriction λ_S have long been known and have been measured as a function of low temperature (Syono 1965; Klerk *et al.* 1977; Kakol *et al.* 1991). It is likely that the stability

(coercivity) of this remanence is often controlled through internal stresses in the titanomagnetite. This is supported by the large size (114×10^{-6}) of λ_S and by internal stresses σ_i that commonly exceed 10^8 Pa in natural titanomagnetites (Appel & Soffel 1984). It is also supported by the observation that coercive force H_C of multidomain titanomagnetite in the two oceanic basalts studied by Hodych (1982a) varies in approximate proportion to λ_S on cooling.

Highly oxidized titanomaghemite dominates in oceanic basalts older than *ca* 10 Myr and is likely the main carrier of the remanence responsible for most oceanic magnetic anomalies (Bleil & Petersen 1983). It has been suggested that the stability of this remanence is magnetostrictively controlled through internal stresses (Housden & O'Reilly 1990), which are inferred to be high from shrinkage cracks in the titanomaghemite (Petersen & Vali 1987). However, this hypothesis has been difficult to test because neither λ_S nor its thermal variation have been measured for titanomaghemite. This is because titanomaghemite is not available in large enough samples for its λ_S to be measured by the conventional methods used for titanomagnetite.

In this paper, we indirectly estimate the saturation magnetostriction λ_S of highly oxidized titanomaghemite typical of oceanic basalts older than *ca* 10 Myr. We use four oceanic basalts containing titanomaghemite ($x \approx 0.55$, $z \approx 0.90$ on average) that is likely mostly in single-domain grains with uniaxial anisotropy resulting from internal stresses. We measure the reversible effect of a small uniaxial compression upon saturation remanence J_{RS} in each basalt. Our measurements are compared with predictions from single-domain theory for this piezomagnetic effect (Bozorth 1951; Hodych 1977) and for H_C (Stoner & Wohlfarth 1948). This yields estimates of λ_S averaging *ca* 6×10^{-6} for the titanomaghemite, which is an order of magnitude less than λ_S for the corresponding titanomagnetite. It also yields estimates of internal stress magnitude σ_i that average *ca* 2×10^8 Pa, which is similar to σ_i inferred for ball-milled single-

domain titanomagnetite with $x \approx 0.6$ (Day *et al.* 1977; O'Reilly 1984 p. 140). Although the effect of uniaxial compression upon magnetization of rocks (including oceanic basalts, Pozzi 1975) has been measured before, we seem to be the first to use the results to estimate λ_S or σ_i .

We also indirectly estimate the low-temperature variation of λ_S using our four oceanic basalts with single-domain titanomaghemite and our one oceanic basalt with pseudo-single-domain titanomaghemite. All five basalts show $H_C J_S$ increasing in approximate proportion to $(1 - \frac{T}{T_C})^n$ with n between 1.9 and 2.0 on cooling to 120 °K (where T is temperature and T_C is Curie point, both in °K). This implies that λ_S for their titanomaghemite ($x \approx 0.55$, $z \approx 0.90$, $T_C \approx 610^\circ\text{K}$ on average) also increases on cooling to 120 °K in approximate proportion to $(1 - \frac{T}{T_C})^n$ with n near 1.9 or 2.0, which is similar to how λ_S increases on cooling in the corresponding titanomagnetite. This supports the hypothesis that magnetostriction commonly controls remanence stability through internal stresses in the highly oxidized titanomaghemites typical of older oceanic basalts, helping preserve the oceanic magnetic anomaly pattern.

2 EXPERIMENTAL METHODS AND RESULTS

2.1 Properties of the titanomaghemite-bearing oceanic basalts

We studied the five oceanic basalts whose hysteresis properties had been measured in fields of up to 5 T by Matzka *et al.* (2003). Four of these (238, 572D, 470A and 556) are likely dominated by single-domain titanomaghemite and one (495) by pseudo-single-domain titanomaghemite. All were from different Ocean Drilling Programme (ODP) sites whose sample codes are given in Table 1. The samples

Table 1. Properties of the rock samples and their magnetic minerals (titanomaghemite in the case of the five oceanic basalts and magnetite in the case of the two continental dolerites). The ODP site code and ocean in which each oceanic basalt was sampled are followed by the age of the basalt. The titanomaghemite in each basalt is described by listing the lattice constant a_0 , Curie point T_C , ratio of titanium to iron atoms Ti/Fe, titanium content parameter x and oxidation parameter z . The ratio of saturation remanence to saturation magnetization J_{RS}/J_S is listed next, followed by J_S . The volume fraction of titanomaghemite in the oceanic basalt is given by F , followed by its 95 per cent confidence interval. The volumetrically average titanomaghemite grain size is given by d . The coercive force is given by H_C . The fractional reversible decrease in J_{RS} per unit of compression parallel to J_{RS} is given by $\frac{1}{\sigma} \frac{\Delta J_{RS}}{J_{RS}}$. When compression is perpendicular to J_{RS} , the effect is smaller by the ratio r and is of opposite sign. The inferred saturation magnetostriction λ_S and internal stress magnitude σ_i are listed last.

Rock type	Oceanic basalts					Dolerites	
Sample	238	572D	470A	556	495	9144	4305
ODP code	238-61-4(6)	572D-34-1(99)	470A-8-3(27)	556-5-2(73)	495-48-4(78)		
Ocean	Indian	Pacific	Pacific	Atlantic	Pacific		
Age (Myr)	34	16	15.7	32	22		
a_0 (Å)	8.379	8.372	8.376	8.376	8.398		
T_C (°C)	365	360	340	305	300	580	580
Ti/Fe	0.242	0.214	0.265	0.274	0.276		
x	0.51	0.50	0.55	0.58	0.57	0	0
z	0.89	0.91	0.90	0.90	0.81	0	0
J_{RS}/J_S	0.44	0.45	0.43	0.50	0.35	0.45	0.42
J_S ($\frac{kA}{m}$)	44	90	39	23	66	480	480
F ($\times 10^{-2}$)	0.94	1.05	1.15	0.83	1.56		
α_{95} ($\times 10^{-2}$)	± 0.22	± 0.20	± 0.34	± 0.24	± 0.54		
d (μm)	2.6	2.2	2.8	2.8	5.4		
H_C (mT)	25.0	37.6	22.3	39.4	12.5	50.4	40.9
$\frac{1}{\sigma} \frac{\Delta J_{RS}}{J_{RS}}$ ($\times 10^{-9} \text{ Pa}^{-1}$)	2.76	2.21	4.58	2.52	3.70	0.65	0.68
r	0.32	0.43	0.30	0.48	0.29	0.38	0.38
λ_S ($\times 10^{-6}$)	4.2	10.4	5.5	3.2		22	19
σ_i ($\times 10^8 \text{ Pa}$)	1.8	2.3	1.1	2.0			

are from three different oceans and range in age from 15.7 to 34 Myr (Table 1). Ages are from Juárez *et al.* (1998) except for sample 572D whose age is from Mayer & Theyer (1985).

Polished sections of each basalt were examined with reflected light microscopy. The main magnetic mineral was identified as titanomaghemite with samples 470A and 495 also containing isolated grains of hemoilmenite. Shrinkage cracks in titanomaghemite (Petersen & Vali 1987) appear in samples 572D, for grains larger than 10 μm , and 495, for grains larger than 18 μm .

The volume fraction F of titanomaghemite was measured for each of the five oceanic basalt cylinders used for stress experiments. This was done by polishing both faces of each basalt cylinder and measuring the fraction of titanomaghemite on each face with the aid of a scanning electron microscope (SEM) operated at 4000 \times magnification in backscatter mode. The fractional area f occupied by titanomaghemite in the $26 \times 23 \mu\text{m}$ area imaged on the SEM screen was measured (as was the size of the titanomaghemite grains). This was repeated for at least 100 positions on each face, evenly spaced to avoid bias. Averaging the resulting >200 measurements of f gives the average F for each cylinder, which is listed in Table 1 along with its 95 per cent confidence interval (estimated from the standard deviation of the >200 measurements of f). The grain-size distribution was used to estimate the volumetrically average grain size (i.e. half the total volume of titanomaghemite is in equal or smaller grains and half in equal or larger grains). Grains less than $\approx 0.5 \mu\text{m}$ across were not measured, being difficult to image in backscatter mode. Even with the finest-grained sample (572D), this should not have led to more than ≈ 10 per cent underestimation of titanomaghemite content, judging by the grain-size distribution. The approximate Ti/Fe ratio of many grains was checked on the SEM using energy-dispersive X-ray (EDX) analysis, to be sure that the bright-appearing grains being measured were titanomaghemite rather than ilmenite, magnetite or pyrite.

For each basalt, the atomic $\frac{\text{Ti}}{\text{Fe}}$ ratio, the lattice constant a_0 and the Curie point T_C were measured for the titanomaghemite to estimate its x and z values (Table 1). The ratio of Ti to Fe atoms was measured for 40 titanomaghemite grains on the polished ends of each oceanic basalt cylinder using the SEM with EDX analysis. The average of the 40 measurements for each basalt should be accurate to within 0.01 with 95 per cent confidence, judging by the standard deviation and by measurements of an ilmenite standard.

Lattice constants a_0 (Table 1) were determined on magnetic extracts that were mixed with SiO_2 powder as a standard. For samples 238 and 572D, a Guinier-type camera was used (Co K_α radiation using an imaging plate in asymmetric back-reflection configuration). For samples 470A, 495, and 556 a diffractometer was used (Mo K_α radiation in transmission).

Curie points T_C were determined using thermomagnetic curves and the method of Grommé *et al.* (1969). The curves were measured for small basalt chips in air in a 400 mT field with a variable field translation balance. For basalts 470A and 556, natural remanence has been thermally demagnetized (fig. 6 of Matzka *et al.* 2003) and shows dominance by the same T_C mineral as in the corresponding high-field thermomagnetic curves.

The composition parameters x and z of the titanomaghemites were estimated from the lattice constant a_0 and the Curie point T_C using the a_0 and T_C contour plots of Readman & O'Reilly (1972). They were also estimated from a_0 and the Ti/Fe atomic ratio assuming oxidation through iron loss and using the a_0 contour plots of Readman & O'Reilly (1972). The average of the two sets of x and z estimates are presented in Table 1. The two sets of x estimates differed on

average by 0.04 and the two sets of z estimates by 0.01. The measurements of Zhou *et al.* (1999) of a_0 versus z in titanomaghemite in oceanic basalts imply that the a_0 contour plots of Readman & O'Reilly (1972) are reasonably reliable (more so than those of Xu *et al.* 1996).

Magnetic hysteresis curves were measured on small basalt chips to a maximum field of 5 T with a Quantum Design Magnetic Properties Measurement System (MPMS, Quantum Design, San Diego, CA, USA). The contribution of paramagnetic minerals to the hysteresis curves was determined using a linear fit between 2 and 5 T and was subtracted from the hysteresis curves before calculating the hysteresis parameters. This yielded the J_{RS}/J_S ratios listed in Table 1 for each of the oceanic basalts. Magnetic hysteresis parameters, including coercive force H_C and saturation magnetization J_S , were also measured in this way as a function of low temperature. These measurements were used to plot the variation of H_C and $H_C J_S$ on cooling for each of the basalts (Fig. 1).

Magnetic hysteresis curves were also measured for each of the oceanic basalt cylinders used for the stress experiments (to reduce error resulting from sample inhomogeneity). A maximum field of 0.28 T in a variable field translation balance was used, yielding the values of H_C listed in Table 1. It also yielded values of J_{RS} per unit volume of basalt for each cylinder. This J_{RS} was divided by the J_{RS}/J_S ratio in Table 1 to give an estimate of the saturation magnetization J_S per unit volume of basalt. This J_S was then divided by F in Table 1 to yield the saturation magnetization J_S per unit volume of titanomaghemite in the basalt cylinder (which is the J_S listed in Table 1). The error in J_S is estimated as ca 30 per cent, most of it ascribed to error in measurement of F .

2.2 Magnetite-bearing continental dolerites

We also studied two magnetite-bearing basaltic samples (9144 and 4305) from two separate dykes in a Mesoproterozoic swarm near Nain, Labrador. Their magnetite is likely dominantly found in single-domain grains (judging by J_{RS}/J_S approaching 0.5) with uniaxial anisotropy provided by grain elongation (judging by H_C showing little change on cooling). The properties of these samples (Table 1) and how they were measured are described in detail by Hodych (1996) and by Hodych *et al.* (1998).

2.3 Stress experiments

For the stress experiments, cylinders of rock 8.7 mm in diameter and 6 to 7 mm in length were prepared. (The cylinder of 470A was only 3 mm long but was extended by gluing on ceramic end pieces.) The ends of each cylinder were ground flat, perpendicular to the cylinder axis. The samples were given a saturation remanence J_{RS} at room temperature in a field of 800 mT either along or perpendicular to the cylinder axis. The stress experiments were conducted inside a magnetic shield with a residual magnetic field of less than 5 nT. A non-magnetic aluminium press (Fig. 2) was used to exert axial compressive stress parallel to the sample's cylinder axis. It is of similar design but smaller than the press described by Hodych (1973). Its special design allows the piston to tilt and provide uniform axial stress, even if the sample's flat ends are not quite parallel. A hand-operated pump was used to compress the oil that pushes down on a 12.7 mm diameter tiltable piston via a rubber diaphragm. The pressure on the 8.7 mm diameter sample should be $\frac{(12.7)^2}{(8.7)^2} \times$ the oil pressure that was measured with a Bourdon gauge (rated accurate to $\frac{1}{2}$ per cent).

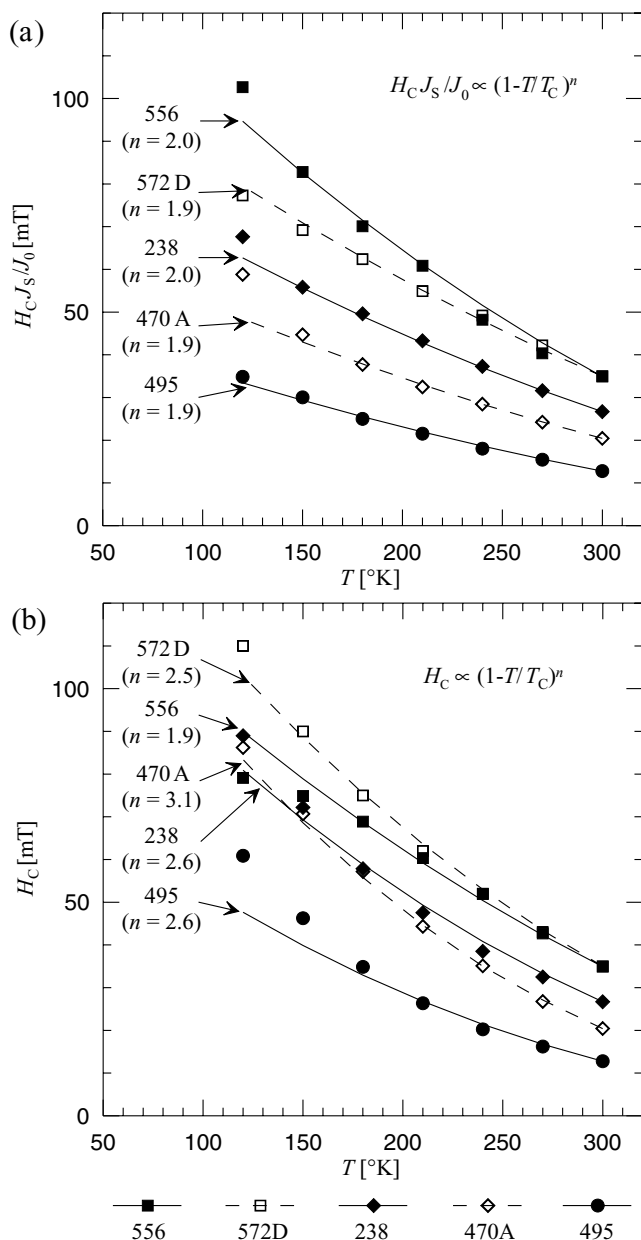


Figure 1. (a) Demonstrating that coercive force H_C multiplied by J_S/J_0 (saturation magnetization divided by its room temperature value) varies in approximate proportion to $(1 - \frac{T}{T_C})^n$ with $n = 1.9$ or 2.0 , on cooling to 120°K for each of our oceanic basalts (where T is temperature and T_C is Curie point, both in $^\circ\text{K}$). The symbols show the observed low-temperature variation of $H_C J_S/J_0$ for each basalt (identified by ODP site, as in Table 1). The curves plot $H_C J_S/J_0$ increasing in proportion to $(1 - \frac{T}{T_C})^n$ on cooling with $n = 1.9$ or 2.0 for each basalt. (b) Testing whether H_C varies in approximate proportion to $(1 - \frac{T}{T_C})^n$ on cooling for each of our basalts. The symbols show the observed low-temperature variation of H_C for each basalt. The curves plot H_C increasing in proportion to $(1 - \frac{T}{T_C})^n$ where n , chosen to fit the observational points, varies from 1.9 to 3.1 for basalts 556 and 470A, respectively.

To determine stress-induced changes in the sample's remanence, relative changes in its magnetic field were measured by a fluxgate probe oriented parallel to the remanence direction. A $\mu\text{MAG-02N}$ fluxgate magnetometer (MacIntyre Electronic Design Associates,

Dulles, VA, USA) with a field neutralization control allowed us to measure field changes as low as 1 nT . In experiments with J_{RS} parallel to the cylinder axis, the probe was mounted in position f1 (second Gaussian position, e.g. Bozorth 1951 p. 839) as indicated in Fig. 2. In experiments with J_{RS} perpendicular to the cylinder axis, the probe was in position f2 (first Gaussian position). Magnetometer drift during each set of experiments was small enough to be ignored (ca 2 nT).

We tested to ensure that compressing a sample did not move it enough to produce magnetic field changes at the probe that could be wrongly interpreted as magnetization changes. An aluminium cylinder of sample size was made and two holes were drilled through its centre, so that one hole was along the cylinder axis and the other hole was perpendicular to the axis. To produce an axial (or a perpendicular) remanence, a magnetized needle was inserted into the axial (or perpendicular) drill hole with plastic modelling material to hold it in place without transmitting stress from the cylinder to the magnetic needle. Compressing this test sample to the maximum stress used with the rock samples resulted in apparent magnetization changes smaller than 0.2 per cent for both axial and perpendicular remanence. Hence, this source of error should be negligible for the rock samples.

For the stress experiments, the samples were subjected to a small base load $\sigma_B = -1.5 \times 10^6\text{ Pa}$ (compressive stress is of negative sign). From that load, an additional compression σ was applied in steps of -4.4×10^6 , -8.8×10^6 , -13.2×10^6 , and then $-17.6 \times 10^6\text{ Pa}$ ($-176 \times 10^6 \frac{\text{dyn}}{\text{cm}^2}$). For each step, the stress was cycled four times between σ_B and $\sigma_B + \sigma$ and the remanence was measured after each pressure change. Stress-induced irreversible changes of remanence were observed only in the first of the four cycles for every step. Hence, only the last three of the four cycles were used to calculate ΔJ_{RS} , the mean reversible part of the remanence change induced by stress σ , which is given by

$$\Delta J_{RS} = J_{RS}(\sigma_B + \sigma) - J_{RS}(\sigma_B). \quad (1)$$

Using a small base load σ_B avoids spurious effects from small sample movements that might occur while the sample seats itself at small loads and has negligible effect on ΔJ_{RS} because the reversible stress-induced remanence change is proportional to σ .

The results of the pressure experiments are shown in Fig. 3 for oceanic basalts 572D and 238 and for the continental dolerite 9144. The observed reversible fractional change in saturation remanence $\Delta J_{RS}/J_{RS}$ is plotted versus the uniaxial stress σ that caused it. The error bars represent an error in the fluxgate reading of ± 1 in the last digit ($\pm 1\text{ nT}$). For all samples, axial compression applied parallel to the remanence direction causes a reversible remanence decrease that is proportional to σ . The slope of the least-squares fit line (through the origin) gives the value of $\frac{1}{\sigma} \frac{\Delta J_{RS}}{J_{RS}}$, the reversible fractional change in J_{RS} per unit stress (listed in Table 1 for each sample). When axial compression is applied perpendicular rather than parallel to the remanence direction, the reversible fractional change in J_{RS} is still proportional to σ but of opposite sign (an increase) and smaller by the factor r (listed in Table 1 for each sample).

An irreversible change in the remanence was observed during the experiments. Unlike the reversible change, the irreversible change was a decrease whether stress was applied parallel or perpendicular to J_{RS} . These irreversible remanence changes were a small percentage of the total remanence (5 per cent at most).

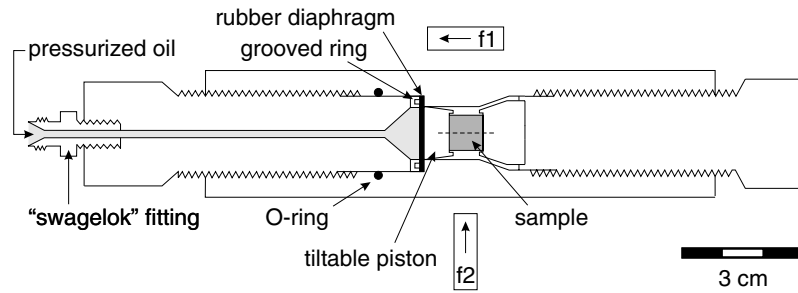


Figure 2. Sketch of the non-magnetic press used for the pressure experiments. The dashed line indicates the sample's cylinder axis. Fluxgate probe positions are labelled f1 and f2 (with arrows indicating the field direction measured).

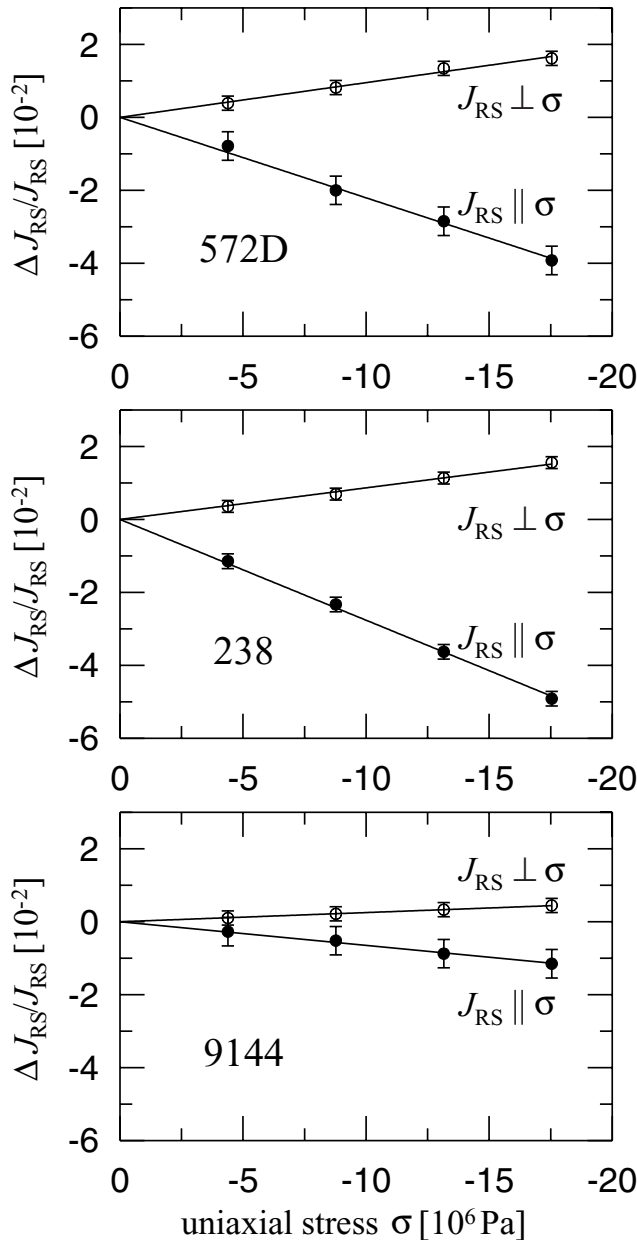


Figure 3. Reversible fractional change $\Delta J_{RS}/J_{RS}$ of saturation remanence under compressive stress σ parallel (filled circles) and perpendicular (open circles) to J_{RS} . Error bars represent ± 1 digit of the magnetometer reading. Least-squares linear fit lines for the data (through the origin) are shown.

3 DISCUSSION

3.1 Saturation magnetization J_S of the titanomaghemite in our oceanic basalts

It is important to reliably determine saturation magnetization J_S of the titanomaghemite in our oceanic basalts because our λ_S estimates for the titanomaghemite are proportional to J_S (as will be shown below). We measured J_S (as outlined above) rather than attempting to estimate it from the composition of the titanomaghemite because J_S may depend strongly upon how the composition was reached. Although the titanomaghemite very likely oxidized through removal of iron rather than addition of oxygen, J_S can depend strongly upon how the removal of iron was partitioned between tetrahedral and octahedral sites (Bleil & Petersen 1983; Matzka *et al.* 2003). The J_S measurements (Table 1) for the titanomaghemite in our five oceanic basalt samples range from 23 to 90 $\frac{kA}{m}$. Most of this variation should be real (because the error in J_S is estimated at only *ca* 30 per cent). The J_S values and their large variation conform to the J_S measurements of Bleil & Petersen (1983) for oceanic basalts of similar T_C .

3.2 Evidence for single-domain titanomaghemite with uniaxial anisotropy resulting from internal stresses in four of our oceanic basalts

Four of our five oceanic basalt samples contain titanomaghemite that is likely mostly in randomly-oriented single-domain grains dominated by uniaxial anisotropy because their J_{RS}/J_S ratio approaches 0.5, as expected theoretically for such grains (Stoner & Wohlfarth 1948). In contrast, the titanomaghemite in oceanic basalt 495 is likely mostly in pseudo-single-domain grains because J_{RS}/J_S is 0.35. This is supported by Bitter pattern observations for 495 showing domain walls in titanomaghemite grains larger than *ca* 5 μm across. Titanomaghemite grains this large dominate 495 (Table 1) but our other four oceanic basalts are dominated by smaller titanomaghemite grains (*ca* 2.2 to 2.8 μm across). The single-domain grains likely dominating these four oceanic basalts possess uniaxial (as a result of the shape or internal stresses) rather than cubic (magnetocrystalline) anisotropy. This is shown by J_{RS}/J_S approaching 0.5 but not the 0.831 (if $K_1 > 0$) or 0.866 (if $K_1 < 0$) expected theoretically (Joffe & Heuberger 1974) for randomly-oriented single-domain titanomaghemite grains dominated by magnetocrystalline anisotropy. (Indeed, none of the 93 oceanic basalt samples studied by Matzka (2001) show J_{RS}/J_S significantly exceeding 0.5 when corrected (Matzka *et al.* 2003) for overestimation of paramagnetism.)

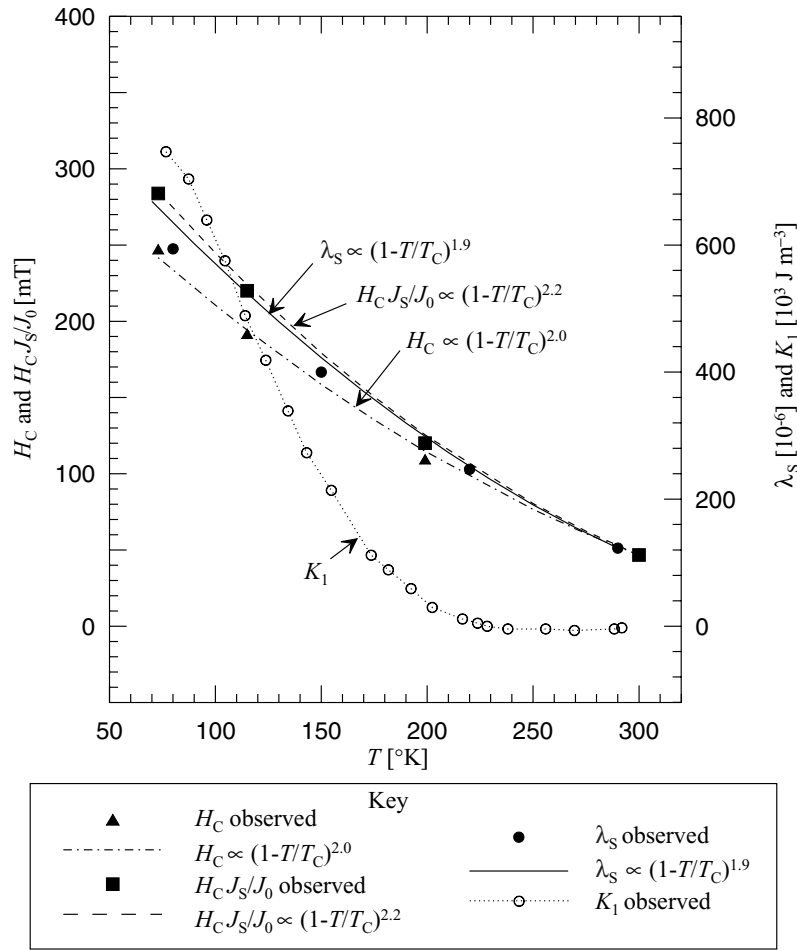


Figure 4. Demonstrating that coercive force H_C of single-domain titanomagnetite ($x = 0.55$) in glass ceramic is very likely controlled by magnetostriction (λ_S) acting through internal stresses, rather than by magnetocrystalline anisotropy (K_1). Also testing whether the low-temperature variation of saturation magnetostriction λ_S can be inferred from that of $H_C J_S$ (where J_S is saturation magnetization). The filled triangles show the observed low-temperature variation of H_C for single-domain grains of titanomagnetite ($x \approx 0.55$, $T_C = 478^\circ\text{K}$) in glass ceramic (from Worm & Markert 1987). The filled squares show the same H_C values multiplied by J_S / J_0 (saturation magnetization J_S divided by its room temperature value J_0 , from the observations of Kakol *et al.* 1991). The dashed-dotted line plots H_C increasing in proportion to $(1 - \frac{T}{T_C})^{2.0}$ on cooling from room temperature (where T is temperature and T_C is Curie point, both in $^\circ\text{K}$). The dashed line plots $H_C J_S / J_0$ increasing in proportion to $(1 - \frac{T}{T_C})^{2.2}$ on cooling from room temperature. The filled circles show the observed low-temperature variation of λ_S for titanomagnetite ($x = 0.56$, $T_C = 443^\circ\text{K}$, from Syono (1965), who notes that λ_S at 80 and 150 $^\circ\text{K}$ is underestimated). The solid line plots λ_S increasing in proportion to $(1 - \frac{T}{T_C})^{1.9}$ on cooling from room temperature. The open circles joined by dotted lines show the observed low-temperature variation of the magnetocrystalline anisotropy constant K_1 for titanomagnetite ($x = 0.56$, $T_C = 443^\circ\text{K}$, from Syono 1965).

It would also be difficult to account for the high coercive force H_C of our oceanic basalts if H_C was dominated by magnetocrystalline anisotropy, as will now be shown. Assuming that the titanomaghemite is in randomly-oriented single-domain grains dominated by cubic magnetocrystalline anisotropy, single-domain theory (Joffe & Heuberger 1974) predicts the following for H_C (in cgs units or for H_C in mT, J_S in $\frac{\text{kA}}{\text{m}}$ and K_1 in $\frac{\text{J}}{\text{m}^3}$):

$$H_C = 0.378 \frac{|K_1|}{J_S} \quad \text{if } K_1 < 0, \tag{2}$$

$$H_C = 0.642 \frac{|K_1|}{J_S} \quad \text{if } K_1 > 0. \tag{3}$$

Rotational hysteresis data (Manson *et al.* 1979) have been used for an indirect estimate of $K_1 \approx 700 \frac{\text{J}}{\text{m}^3}$ for titanomaghemite with $x = 0.6$ and $z = 0.8$ (Moskowitz 1980). This is likely an overestimate of K_1 because it neglects the contribution of internal stresses to

rotational hysteresis (as discussed below). Substituting this value of K_1 and $J_S = 49 \frac{\text{kA}}{\text{m}}$ (the average J_S for our four single-domain titanomaghemites) into eqs (2) and (3) predicts $H_C = 5.4$ mT if $K_1 < 0$ and $H_C = 9.2$ mT if $K_1 > 0$. The average H_C of 31 mT observed for our four basalts with single-domain titanomaghemite is much greater than either of these predictions, making magnetocrystalline control of their H_C unlikely. (Pseudo-single-domain titanomaghemite with magnetocrystalline control of H_C might fortuitously give J_{RS} / J_S near 0.5, but its H_C should be even smaller than 5.4 or 9.2 mT).

Having shown that four of our basalts are very likely dominated by randomly-oriented single-domain titanomaghemite grains with uniaxial anisotropy, we consider whether the uniaxial anisotropy is the result of grain elongation or internal stresses. Assuming that the uniaxial anisotropy is the result of grain elongation (with N_b and N_a the self-demagnetizing factors across and along the long axis of the

single-domain grain, respectively), single-domain theory (Stoner & Wohlfarth 1948) predicts the following for H_C (in cgs units with $\mu_0 = 1$, or for H_C in mT, J_S in $\frac{\text{kA}}{\text{m}}$ and $\mu_0 = 4\pi \times 10^{-7} \frac{\text{H}}{\text{m}}$):

$$H_C = 0.479\mu_0(N_b - N_a)J_S. \quad (4)$$

Even if the titanomaghemite grains were extremely elongated so that $N_b - N_a = 0.5$ (2π in cgs units), eq. (4) with average $J_S = 49 \frac{\text{kA}}{\text{m}}$ predicts that average H_C resulting from shape anisotropy should not exceed 15 mT. This is much less than the average H_C of 31 mT observed in these basalts (Table 1). Furthermore, for all five of our oceanic basalts, we observe that cooling from 300 to 120 °K causes a large increase in H_C (Fig. 1b) whereas J_S decreases (J_S versus T is not plotted explicitly, but can be derived from Fig. 1). Certainly H_C does not vary in proportion to J_S as expected from eq. (4), ruling out control of H_C by shape anisotropy. Hence, λ_S control of H_C seems the only viable option and the way H_C varies on cooling very likely reflects how λ_S varies on cooling as will be discussed in Section 3.5.

3.3 Inferring λ_S for single-domain titanomaghemite in our oceanic basalts

For all five of our titanomaghemite-bearing basalt samples, J_{RS} decreases reversibly when compressed parallel to J_{RS} (Fig. 3). This shows that λ_S must be positive for their highly oxidized titanomaghemites, as is the case for titanomagnetite ($x \approx 0.6$) and magnetite. This is not a trivial result because λ_S is negative for maghemite (Dunlop & Özdemir 1997, p. 51).

Average magnetostriction λ_S can be indirectly estimated for randomly-oriented single-domain grains with uniaxial anisotropy from measurements of $\frac{1}{\sigma} \frac{\Delta J_{RS}}{J_{RS}}$ (the reversible fractional change in J_{RS} per unit of small axial compression σ applied parallel to J_{RS}) by using the following equation (in cgs units or for H_C in mT, J_S in $\frac{\text{kA}}{\text{m}}$ and σ in Pa):

$$\lambda_S = 1.39H_CJ_S \frac{1}{\sigma} \frac{\Delta J_{RS}}{J_{RS}}. \quad (5)$$

Eq. (5) is valid whether the uniaxial anisotropy of the single-domain grains is the result of grain elongation or internal stresses, as we shall now show. Assuming the uniaxial anisotropy is the result of grain elongation, eq. (5) can be derived by combining eq. (4) with the following theoretical expression (Hodoch 1977) for $\frac{1}{\sigma} \frac{\Delta J_{RS}}{J_{RS}}$ (in cgs units with $\mu_0 = 1$, or for J_S in $\frac{\text{kA}}{\text{m}}$ and σ in Pa with $\mu_0 = 4\pi \times 10^{-7} \frac{\text{H}}{\text{m}}$):

$$\frac{1}{\sigma} \frac{\Delta J_{RS}}{J_{RS}} = \frac{3}{2} \frac{\lambda_S}{\mu_0(N_b - N_a)J_S^2}. \quad (6)$$

Assuming the uniaxial anisotropy is the result of internal stresses σ_i in the single-domain grains, eq. (5) can be derived by combining the following theoretical expressions for H_C (Stoner & Wohlfarth 1948) and $\frac{1}{\sigma} \frac{\Delta J_{RS}}{J_{RS}}$ (Bozorth 1951, p. 625) valid for cgs units or for H_C in mT, J_S in $\frac{\text{kA}}{\text{m}}$ and σ in Pa:

$$H_C = 1.437 \frac{\lambda_S \sigma_i}{J_S}, \quad (7)$$

$$\frac{1}{\sigma} \frac{\Delta J_{RS}}{J_{RS}} = \frac{1}{2\sigma_i}. \quad (8)$$

Assuming that the easy axes of the elongated or stressed grains are randomly oriented relative to crystallographic axes, the average saturation magnetostriction estimated by eq. (5) should equal $\lambda_S = \frac{2}{5}\lambda_{100} + \frac{3}{5}\lambda_{111}$ (Bozorth 1951, p. 652) where λ_{100} and λ_{111}

are saturation magnetostriction along the [100] and [111] axis, respectively.

Substituting the observed H_C , $\frac{1}{\sigma} \frac{\Delta J_{RS}}{J_{RS}}$ and J_S into eq. (5) yields indirect estimates of λ_S for the single-domain titanomaghemite dominating oceanic basalts 238, 572D, 470A and 556 (Table 1). There could be large errors in these estimates of λ_S . Underestimation of λ_S could result from not all of the titanomaghemite being in single-domain grains as suggested by J_{RS}/J_S being on average 0.46 rather than the 0.50 expected from single-domain theory. It is also suggested by the ratio r (Table 1) being on average 0.38 rather than the 0.50 expected from single-domain theory (Hodoch 1977). On the other hand, overestimation of λ_S could result from our assumption that the average uniaxial compression σ delivered to the titanomaghemite grains is the same as that applied to the basalt sample. The compression could be significantly higher if titanomaghemite (like magnetite) is more rigid than the basalt as a whole (Hamano 1983).

To determine how much error is likely in our λ_S estimate for titanomaghemite, we estimated λ_S in the same way for magnetite. Magnetite is likely to yield higher error in λ_S estimation by our method because its magnetostriction is uncommonly anisotropic ($\lambda_{100} = -19.5 \times 10^{-6}$, $\lambda_{111} = 72.6 \times 10^{-6}$). We used the two basaltic dyke samples (9144 and 4305), which had the highest J_{RS}/J_S (=0.45 and 0.42, respectively) of a suite of magnetite-bearing Precambrian dykes from Nain, Labrador. Because J_{RS}/J_S approaches 0.50 and H_C shows little change on cooling to 77 °K, the magnetite in both 9144 and 4305 is likely mostly in single-domain grains dominated by uniaxial anisotropy provided by grain elongation (Hodoch 1996). Because the magnetite is intergrown with ilmenite lamellae exsolved along {111} planes, the magnetite grains are likely elongated along [110] directions. Magnetic interaction between these elongated grains can likely be ignored in first approximation (Hodoch 1996). Substituting H_C , $\frac{1}{\sigma} \frac{\Delta J_{RS}}{J_{RS}}$ and J_S from Table 1 into eq. (5) yields indirect estimates of $\lambda_S = 22 \times 10^{-6}$ and 19×10^{-6} for 9144 and 4305, respectively. Although these are on average 43 per cent less than $\frac{2}{5}\lambda_{100} + \frac{3}{5}\lambda_{111}$ for magnetite, they are on average only 23 per cent less than $\frac{1}{2}(\lambda_{111} + \lambda_{100})$, which is the λ_S expected if the magnetite grains are elongated along [110] instead of along random crystallographic directions (Hodoch 1977). This suggests that our λ_S estimates for titanomaghemite in samples 572D, 238, 556 and 470A are likely within ca 50 per cent of the true value (taking into account additional error contributed by J_S).

Our experimental estimate of average λ_S is ca 6×10^{-6} for titanomaghemite with $x \approx 0.55$ and $z \approx 0.9$. This is much higher than the $ca 1 \times 10^{-6}$ expected if λ_S varies in approximate proportion to $(1 - z)^2$ as predicted by Housden & O'Reilly (1990). However, they point out that their prediction neglects the contribution of Fe^{3+} ions to λ_S and should increasingly underestimate λ_S as z approaches 1. Moskowitz (1980) used rotational hysteresis data (Manson *et al.* 1979) to estimate how K_1 varies with z in titanomaghemite and then assumed that λ_S varies in proportion to K_1 . However, the rotational hysteresis data of the synthetic single-domain titanomaghemites of Manson *et al.* (1979) are more likely dominated by λ_S acting through internal stresses rather than by K_1 . This is because the titanomaghemites were prepared by wet grinding in a ball mill for four days. In titanomagnetites ($x \approx 0.6$) this typically produces single-domain grains whose coercive force is too high to be the result of shape or magnetocrystalline anisotropy and is thought to be the result of magnetostriction acting through internal stresses that would have to be ca 1×10^8 Pa in magnitude. Assuming that this is also true of the single-domain titanomaghemites of Manson *et al.* (1979), the rotational hysteresis magnitudes reported would

imply $\lambda_S \approx 4 \times 10^{-6}$ for titanomaghemite with $x = 0.5, z = 0.8$ or with $x = 0.6, z = 0.84$. This follows from peak rotational hysteresis per unit volume per cycle $W_{rp} = 1.8(\frac{3}{2}\lambda_S\sigma_i)$ for randomly-oriented single-domain grains with uniaxial anisotropy resulting from stress according to theory by Jacobs & Luborsky (1957), using cgs units or W_{rp} in $\frac{J}{m^3}$ and σ_i in Pa. This estimate is in reasonable agreement with our average λ_S estimate, but our estimate has the advantage of not needing to assume that the internal stress magnitude is $\approx 1 \times 10^8$ Pa.

3.4 Inferring internal stress magnitude for single-domain titanomaghemite in our oceanic basalts

We have shown that oceanic basalts 572D, 238, 556 and 470A are very likely dominated by single-domain titanomaghemite with uniaxial anisotropy resulting from internal stresses. Hence, we can use eq. (8) and measurements of $\frac{1}{\sigma} \frac{\Delta J_{RS}}{J_{RS}}$ to infer the internal stress magnitude σ_i in their single-domain titanomaghemites. These σ_i estimates (Table 1) range from 1.1×10^8 to 2.3×10^8 Pa with average $\sigma_i = 1.8 \times 10^8$ Pa. The error in estimating σ_i is independent of error in J_S and may be similar to the *ca* 23 per cent error in estimating λ_S of single-domain magnetite in our dolerites from measurements of $\frac{1}{\sigma} \frac{\Delta J_{RS}}{J_{RS}}$.

Internal stress $\sigma_i \approx 1.8 \times 10^8$ Pa is not unreasonably high because a similar internal stress magnitude is assumed to explain the high coercivity of single-domain haematite (Porath 1968; Dunlop & Özdemir 1997 p. 72) and the high coercivity of ball-milled titanomagnetite with $x = 0.6$ (Day *et al.* 1977; O'Reilly 1984 p. 140). For large multidomain titanomaghemite grains ($x \approx 0.6, z < 0.6$), Appel (1987) estimated the internal stress magnitude to average *ca* 5×10^7 Pa. It seems likely that the much higher internal stresses in our titanomaghemites with higher oxidation degree are the result of shrinking of the crystal lattice during low-temperature oxidation. This is thought to produce the severe cracking observed for titanomaghemite particles greater than *ca* $5 \mu\text{m}$ (Petersen & Vali 1987). Housden & O'Reilly (1990) suggested that titanomaghemite grains smaller than the threshold of shrinkage crack formation deform plastically and that their internal stress is comparable to that of ball-milled titanomagnetites. They assumed internal stresses of *ca* 2×10^8 Pa for the small titanomaghemite grains that are important carriers of natural remanence in oceanic basalts. Our estimates of σ_i support this assumption.

3.5 Inferring how λ_S varies upon cooling for titanomaghemite in our oceanic basalts

Having shown that oceanic basalts 572D, 238, 556 and 470A are very likely dominated by single-domain titanomaghemite whose H_C is magnetostrictively controlled by internal stress, we expect that eq. (7) applies and that H_C should vary in proportion to $\frac{2\lambda_S\sigma_i}{J_S}$ upon cooling from room temperature. Approximately the same is expected theoretically if the titanomaghemite is in pseudo-single-domain grains (as in oceanic basalt 495) or multidomain grains, provided that opposition to domain wall motion is magnetostrictively controlled through internal stresses (Hodych 1982b). Hence, measuring how $H_C J_S$ varies upon cooling in our oceanic basalts should allow us to infer how λ_S of their titanomaghemite varies upon cooling. This assumes that internal stresses remain approximately constant upon cooling. This assumption seems justified for magnetite because $H_C J_S$ commonly varies in approximate propor-

tion to λ_S for multidomain and pseudo-single-domain magnetite (Hodych 1982a; Hodych *et al.* 1998).

The assumption that internal stresses remain approximately constant on cooling also seems justified for titanomagnetite ($x \approx 0.55$), as will now be shown. For single-domain titanomagnetite ($x \approx 0.55, T_C = 205^\circ\text{C}$) in glass ceramic, Worm & Markert (1987) showed that H_C increases on cooling similarly to λ_S (and unlike K_1). This can be seen in Fig. 4 where these H_C data are plotted along with data for λ_S and K_1 from Syono (1965) for synthetic titanomagnetite ($x = 0.56, T_C = 170^\circ\text{C}$). Hence, it is very likely that H_C is magnetostrictively controlled through internal stresses. The variation of $H_C J_S$ is also shown (using J_S data for $x = 0.55$ titanomagnetite from Kakol *et al.* 1991) and is similar to that of H_C because J_S shows relatively little variation on cooling. Both $H_C J_S$ and λ_S vary on cooling in approximate proportion to $(1 - \frac{T}{T_C})^n$ where $n = 2.2$ for $H_C J_S$ and $n = 1.9$ for λ_S (where T is temperature and T_C is Curie point, both in $^\circ\text{K}$). The difference in *n* of *ca* 0.3 gives an estimate of the error expected if one assumes that σ_i remains constant on cooling and infers the low-temperature variation of λ_S from that of $H_C J_S$ in single-domain titanomagnetite with $x \approx 0.55$. Note that the power-law exponent *n* is sensitive to error in T_C . We used the λ_S data of Syono (1965) rather than that of Klerk *et al.* (1977) because the latter implied unusually low T_C values. Above room temperature, λ_S obeys the same power law but the exponent $n = 1.3$ for titanomagnetite with $x = 0.6$ or 0.4 , as shown by Moskowitz (1993).

For all five of our oceanic basalts, cooling from room temperature to 120°K causes $H_C J_S$ to increase in approximate proportion to $(1 - \frac{T}{T_C})^n$ with *n* between 1.9 and 2.0. This is shown in Fig. 1(a), whose curves were drawn by assuming that $H_C J_S$ for a given basalt would increase upon cooling from room temperature in approximate proportion to $(1 - \frac{T}{T_C})^n$ where T_C is the Curie point measured for that basalt (Table 1). Various values of *n* were tried (in increments of 0.1) and for each basalt the best fit to the observational data points was obtained with $n = 1.9$ or 2.0 .

For the four oceanic basalts dominated by single-domain titanomaghemite, this observed increase of $H_C J_S$ on cooling implies (eq. 7) that λ_S also increases in proportion to $(1 - \frac{T}{T_C})^n$ with *n* near 1.9 or 2.0 on cooling from room temperature to 120°K . This assumes that internal stresses σ_i remain constant, which may cause an error of *ca* 0.3 in the power-law exponent, judging by the behaviour of single-domain titanomagnetite with $x \approx 0.55$. The fifth oceanic basalt (495) is dominated by pseudo-single-domain titanomaghemite whose $H_C J_S$ behaves similarly, suggesting that its λ_S varies in approximate proportion to $(1 - \frac{T}{T_C})^{1.9}$ on cooling from room temperature to 120°K .

Housden & O'Reilly (1990) suggested that H_C would vary with temperature in approximate proportion to $(1 - \frac{T}{T_C})^{2.4}$ for single-domain and perhaps multidomain titanomaghemites with $x \approx 0.6$ in oceanic basalts. As shown in Fig. 1(b) for our oceanic basalts, H_C varies in approximate proportion to $(1 - \frac{T}{T_C})^n$ on cooling to 120°K . However, the observed H_C data points do not fit this power law as well as $H_C J_S$ does. Also, *n* is not as constant as with $H_C J_S$, but varies from 1.9 to 3.1, because of variation in the way J_S decreases on cooling from basalt to basalt. This varied behaviour of J_S is consistent with evidence (Matzka *et al.* 2003) that the titanomaghemite is a ferrimagnet of P-type (Néel 1948) in basalts 238, 556 and 572D and of N-type in basalts 470A and 495.

Our observations suggest that $H_C J_S$ commonly varies in approximate proportion to $(1 - \frac{T}{T_C})^n$ on cooling with *n* showing little variation from 1.9 or 2.0 for single-domain (and perhaps pseudo-single-domain) natural titanomaghemites with $x \approx 0.55$ and $z \approx 0.9$. As shown above, this variation of $H_C J_S$ on cooling is very likely the

result of H_C being magnetostrictively controlled by internal stresses in the titanomaghemites. Our results support the hypothesis (Housden & O'Reilly 1990) that internal stresses in titanomaghemites are an important source of magnetic stability in oceanic basalts, helping preserve the oceanic magnetic anomaly pattern. We suggest testing this hypothesis further by extensive observation of whether it is common for $H_C J_S$ of such basalts to vary on cooling in approximate proportion to $(1 - \frac{T}{T_C})^n$ with $n \approx 1.9$ or 2.0 .

One could similarly test the proposal of Gee & Kent (1995) that magnetocrystalline anisotropy rather than internal stresses may commonly dominate coercivity in the relatively unoxidized titanomagnetites of basalts on mid-ocean ridges. They proposed this to explain why their J_{RS}/J_S estimates often significantly exceeded 0.5 in their mid-ocean-ridge basalt samples. However, this may be an artefact of their using a maximum field of only 1 T, causing serious overestimation of J_{RS}/J_S , as was demonstrated for our titanomaghemite-bearing oceanic basalts by Matzka *et al.* (2003). The importance of internal stress control of coercivity in mid-ocean-ridge basalts would be supported if $H_C J_S$ of the basalts was found to commonly vary in approximate proportion to λ_S rather than K_1 on cooling. This variation with λ_S has been observed in the two oceanic basalts bearing multidomain titanomagnetite studied by Hodych (1982a). However, corresponding data for oceanic basalts bearing single-domain or pseudo-single-domain titanomagnetite are lacking.

4 CONCLUSIONS

(i) For a sample of coercive force H_C dominated magnetically by randomly-oriented single-domain grains with uniaxial anisotropy and saturation magnetization J_S , theory predicts that the reversible change ΔJ_{RS} in saturation remanence caused by applying a small axial stress σ parallel to J_{RS} should yield an estimate of saturation magnetostriction λ_S given by eq. (5): $\lambda_S = 1.39 H_C J_S \frac{1}{\sigma} \frac{\Delta J_{RS}}{J_{RS}}$.

(ii) We describe a small non-magnetic press and how it was used with a fluxgate magnetometer in field-free space to measure $\frac{1}{\sigma} \frac{\Delta J_{RS}}{J_{RS}}$, the reversible fractional change in saturation remanence per unit of compression applied parallel to the remanence direction of our rock samples.

(iii) The estimate of λ_S given by eq. (5) was tested by measuring $\frac{1}{\sigma} \frac{\Delta J_{RS}}{J_{RS}}$ for two basaltic samples containing single-domain magnetite grains (with uniaxial anisotropy) intergrown with ilmenite lamellae. Eq. (5) yielded λ_S estimates of 19 and 22×10^{-6} . This is in satisfactory agreement with directly measured values of λ_{111} and λ_{100} , because it is on average only *ca* 23 per cent lower than the $\lambda_S = \frac{1}{2}(\lambda_{111} + \lambda_{100})$ expected for single-domain magnetite elongated along [110] directions by ilmenite exsolution lamellae.

(iv) In the same way, λ_S was estimated for titanomaghemite (with titanium content parameter $x \approx 0.55$ and oxidation parameter $z \approx 0.90$) by measuring $\frac{1}{\sigma} \frac{\Delta J_{RS}}{J_{RS}}$ for four oceanic basalt samples dominated by single-domain titanomaghemite grains with uniaxial anisotropy. Eq. (5) gives estimates of λ_S that should be within 50 per cent of the true values, where $\lambda_S = \frac{2}{3}\lambda_{100} + \frac{3}{5}\lambda_{111}$ (assuming the easy axes of the grains are along random crystallographic directions). The estimates of λ_S range from 3×10^{-6} to 10×10^{-6} and their average is 6×10^{-6} .

(v) We show that the uniaxial anisotropy in the single-domain titanomaghemite grains dominating four of our oceanic basalts is very likely the result of internal stresses σ_i . The magnitude of σ_i was estimated using eq. (8): $\frac{1}{\sigma} \frac{\Delta J_{RS}}{J_{RS}} = \frac{1}{2\sigma_i}$. This yields $\sigma_i \approx 2 \times 10^8$ Pa on average, which is similar in magnitude to the σ_i thought

to be responsible for the high coercivity of natural single-domain haematite and ball-milled single-domain titanomagnetite ($x = 0.6$).

(vi) For each of our four oceanic basalts dominated by single-domain titanomaghemite, $H_C J_S$ varies on cooling to 120 °K in approximate proportion to $(1 - \frac{T}{T_C})^n$ with n between 1.9 and 2.0. This implies that λ_S of the titanomaghemite ($x \approx 0.55$, $z \approx 0.90$) also varies on cooling in approximate proportion to $(1 - \frac{T}{T_C})^n$ with $n \approx 1.9$ or 2.0 (assuming that internal stresses remain constant on cooling, which may cause an error of *ca* 0.3 in the power-law exponent). This is similar to the variation of λ_S on cooling in the corresponding titanomagnetite.

(vii) Our results support the hypothesis that it is common for coercivity to be magnetostrictively controlled by internal stresses in the highly oxidized titanomaghemites typical of oceanic basalts older than *ca* 10 Myr, helping preserve the oceanic magnetic anomaly pattern. To test this hypothesis further, we suggest more extensive observation of whether $H_C J_S$ of such basalts does commonly vary in approximate proportion to $(1 - \frac{T}{T_C})^n$ with n near 1.9 or 2.0, on cooling to 120 °K.

ACKNOWLEDGMENTS

The authors thank N. Petersen and H. C. Soffel for helpful discussions. The Ocean Drilling Programme provided the oceanic basalt samples. The authors were very ably assisted in the laboratory by D. Krasa and J. Schneider (determining lattice constants) and by M.P. Wheeler (determining titanomaghemite content). The low-temperature hysteresis measurements were conducted at the Institute for Rock Magnetism, which is funded by the Keck Foundation, National Science Foundation and University of Minnesota. The stress experiments were conducted with the help of a grant to JPH from the Natural Sciences and Engineering Research Council of Canada. JM gratefully acknowledges financial support from the Deutsche Forschungsgemeinschaft. The authors thank B. Moskowitz and one anonymous reviewer for helpful comments on the manuscript.

REFERENCES

- Appel, E., 1987. Stress anisotropy in Ti-rich titanomagnetites, *Phys. Earth planet. Int.*, **46**, 233–240.
- Appel, E. & Soffel, H.C., 1984. Model for the domain state of Ti-rich titanomagnetites, *Geophys. Res. Lett.*, **11**, 189–192.
- Bleil, U. & Petersen, N., 1983. Variations in magnetization intensity and low-temperature titanomagnetite oxidation of ocean floor basalts, *Nature*, **301**, 384–388.
- Bozorth, R.M., 1951. *Ferromagnetism*, Van Nostrand, New York.
- Day, R., Fuller, M.D. & Schmidt, V.A., 1977. Hysteresis properties of titanomagnetites: Grain size and composition dependence, *Phys. Earth planet. Int.*, **13**, 260–267.
- Dunlop, D.J. & Özdemir, Ö., 1997. *Rock Magnetism: Fundamentals and Frontiers*, Cambridge Studies in Magnetism series, Cambridge University Press, Cambridge.
- Gee, J. & Kent, D.V., 1995. Magnetic hysteresis in young mid-ocean ridge basalts: Dominant cubic anisotropy?, *Geophys. Res. Lett.*, **22**, 551–554.
- Grommé, C.S., Wright, T.L. & Peck, D.L., 1969. Magnetic properties and oxidation of iron-titanium oxide minerals in Alae and Makaopuhi Lava Lakes, Hawaii, *J. geophys. Res.*, **74**, 5277–5293.
- Hamano, Y., 1983. Experiments on the stress sensitivity of natural remanent magnetization, *J. Geomag. Geoelectr.*, **35**, 155–172.
- Hodych, J.P., 1973. A nonmagnetic uniaxial press with a tiltable piston, *J. Phys. Earth*, **6**, 1037–1039.
- Hodych, J.P., 1977. Single-domain theory of the reversible effect of small uniaxial stress upon the remanent magnetization of rock, *Can. J. Earth. Sci.*, **14**, 2047–2061.

- Hodych, J.P., 1982a. Magnetic hysteresis as a function of low temperature for deep-sea basalts containing large titanomagnetite grains—interference of domain state and controls on coercivity, *Can. J. Earth Sci.*, **19**, 144–152.
- Hodych, J.P., 1982b. Magnetostrictive control of coercive force in multidomain magnetite, *Nature*, **298**, 542–544.
- Hodych, J.P., 1996. Inferring domain state from magnetic hysteresis in high coercivity dolerites bearing magnetite with ilmenite lamellae, *Earth planet. Sci. Lett.*, **142**, 523–533.
- Hodych, J.P., Mackay, R.I. & English, G.M., 1998. Low-temperature demagnetization of saturation remanence in magnetite-bearing dolerites of high coercivity, *Geophys. J. Int.*, **132**, 401–411.
- Housden, J. & O'Reilly, W., 1990. On the intensity and stability of the natural remanent magnetization of ocean floor basalts, *Phys. Earth planet. Int.*, **64**, 261–278.
- Irving, E., 1970. The Mid-Atlantic-Ridge at 45°N. XIV. Oxidation and magnetic properties of basalts; review and discussion, *Can. J. Earth Sci.*, **7**, 1528–1538.
- Jacobs, I.S. & Luborsky, F.E., 1957. Magnetic anisotropy and rotational hysteresis in elongated fine-particle magnets, *J. appl. Phys.*, **28**, 467–473.
- Joffe, I. & Heuberger, R., 1974. Hysteresis properties of distributions of cubic single-domain ferromagnetic particles, *Phil. Mag.*, **29**, 1051–1059.
- Johnson, H.P. & Hall, J.M., 1978. A detailed rock magnetic and opaque mineralogy study of the basalts from the Nazca Plate, *Geophys. J. R. astr. Soc.*, **52**, 45–64.
- Juárez, M.T., Tauxe, L., Gee, J. & Pick, T., 1998. The intensity of the Earth's magnetic field of the past 160 million years, *Nature*, **394**, 878–881.
- Kakol, Z., Sabol, J. & Honig, J.M., 1991. Magnetic anisotropy of titanomagnetites $\text{Fe}_{3-x}\text{Ti}_x\text{O}_4$, $0 \leq x \leq 0.55$, *Phys. Rev. B*, **44**, 2198–2204.
- Klerk, J., Brabers, V.A. & Kuipers, A.J.M., 1977. Magnetostriction of the mixed series $\text{Fe}_{3-x}\text{Ti}_x\text{O}_4$, *J. Physique*, **38**, 187–189.
- Manson, A.J., O'Donovan, J.B. & O'Reilly, W., 1979. Magnetic rotational hysteresis loss in titanomagnetites and titanomaghemites—application to non-destructive mineral identification in basalts, *J. Geophys.*, **46**, 185–199.
- Matzka, J., 2001. Besondere magnetische Eigenschaften der Ozeanbasalte im Altersbereich 10 bis 40 Ma, *PhD thesis*, Ludwig-Maximilians-Universität München, Munich.
- Matzka, J., Krása, D., Kunzmann, T. & Petersen, N., 2003. Magnetic state of 10–40 Ma old ocean basalts and its implication for natural remanent magnetization, *Earth planet. Sci. Lett.*, **206**, 541–553.
- Mayer, L. & Theyer, F., 1985. *Initial Reports DSDP, 85*, U.S. Govt. Printing Office, Washington.
- Moskowitz, B.M., 1980. Theoretical grain size limits for single-domain, pseudo-single-domain and multi-domain behavior in titanomagnetite ($x = 0.6$) as a function of low-temperature oxidation, *Earth planet. Sci. Lett.*, **47**, 285–293.
- Moskowitz, B.M., 1993. High temperature magnetostriction of magnetite and titanomagnetite, *J. geophys. Res.*, **98**, 359–371.
- Néel, M.L., 1948. Propriétés magnétiques des ferrites; ferrimagnétisme et antiferromagnétisme, *Annales de Physique*, **12**(3), 137–198.
- O'Reilly, W., 1984. *Rock and Mineral Magnetism*, Blackie & Son, Glasgow and London.
- O'Reilly, W. & Banerjee, S.K., 1966. The mechanism of oxidation in titanomagnetites and self-reversal, *Nature*, **221**, 26–28.
- Petersen, N. & Vali, H., 1987. Observation of shrinkage cracks in ocean floor titanomagnetites, *Phys. Earth planet. Int.*, **46**, 197–205.
- Petersen, N., Eisenach, P. & Bleil, U., 1979. Low temperature alteration of the magnetic minerals in ocean floor basalts, in *Deep Drilling Results in the Atlantic Ocean: Ocean Crust*, Vol. 2 of, eds Talwani, M., Harrison, C.G. & Hayes, D.E., pp. 169–209. American Geophysical Union, Washington.
- Porath, H., 1968. Stress induced magnetic anisotropy in natural single crystals of hematite, *Phil. Mag.*, **17**, 603–608.
- Pozzi, J.P., 1975. Magnetic properties of oceanic basalts—effects of pressure and consequences for the interpretation of magnetic anomalies, *Earth planet. Sci. Lett.*, **26**, 337–344.
- Prévot, M., Remond, G. & Caye, R., 1968. Étude de la transformation d'une titanomagnétite en titanomaghémite dans une roche volcanique, *Bulletin de la Société Française de Minéralogie et de Cristallographie*, **91**, 65–74.
- Readman, P. & O'Reilly, W., 1972. Magnetic properties of oxidized (cation-deficient) titanomagnetites (Fe , Ti , \square) $_3\text{O}_4$, *J. Geomag. Geoelectr.*, **24**, 69–90.
- Stoner, E.C. & Wohlfarth, E.P., 1948. A mechanism of magnetic hysteresis in heterogeneous alloys, *Phil. Trans. R. Soc. Lond., A.*, **240**, 599–642.
- Syono, Y., 1965. Magnetocrystalline anisotropy and magnetostriction of Fe_3O_4 — Fe_2TiO_4 series—with special application to rock magnetism, *Jap. J. Geophys.*, **4**, 71–143.
- Worm, H.U. & Markert, H., 1987. Magnetic hysteresis properties of fine particle titanomagnetites precipitated in a silicate matrix, *Phys. Earth planet. Int.*, **46**, 84–92.
- Xu, W., Peacor, D.R., Van der Voo, R., Dolase, W. & Beaubouef, R.T., 1996. Modified lattice parameter/Curie temperature diagrams for titanomagnetite/titanomaghemite within the quadrilateral Fe_3O_4 — Fe_2TiO_4 — Fe_2O_3 — Fe_2TiO_5 , *Geophys. Res. Lett.*, **23**, 2811–2814.
- Zhou, W., Peacor, D.R. & Van der Voo, R., 1999. Determination of lattice parameter, oxidation state, and composition of individual titanomagnetite/titanomaghemite grains by transmission electron microscopy, *J. geophys. Res.*, **104**, 17 689–17 702.